

# Affine extensions of the icosahedral group with applications to the three-dimensional organisation of simple viruses

T. Keef<sup>1</sup> and R. Twarock<sup>1,2</sup>

<sup>1</sup>*Department of Mathematics  
University of York*

<sup>2</sup>*Department of Biology  
University of York  
York YO10 5DD, U.K.*

## Abstract

Since the seminal work of Caspar and Klug on the structure of the protein containers that encapsulate and hence protect the viral genome, it has been recognised that icosahedral symmetry is crucial for the structural organisation of viruses. In particular, icosahedral symmetry has been invoked in order to predict the surface structures of viral capsids in terms of tessellations or tilings that schematically encode the locations of the protein subunits in the capsids. Whilst this approach is capable of predicting the relative locations of the proteins in the capsids, information on their tertiary structures and the organisation of the viral genome within the capsid are inaccessible. We develop here a mathematical framework based on affine extensions of the icosahedral group that allows us to describe those aspects of the three-dimensional structure of simple viruses. This approach complements Caspar Klug Theory and provides details on virus structure that have not been accessible with previous methods, implying that icosahedral symmetry is more important for virus architecture than previously appreciated.

## 1 Introduction

An important constituent of a virus is its protein container, called the viral capsid. It packages the genomic material, either RNA or DNA, and transports it into a host cell like a Trojan horse, hijacking the host's cellular mechanism to produce new viruses. Crick and Watson observed in 1956 that the size of the packaged genomic material is too small to encode for more than a limited number of different capsid proteins. Based on this observation they argued that viruses must be formed from identical capsid proteins that are organised according to symmetry [1]. Subsequent experiments confirmed this conjecture, showing that most viruses exhibit icosahedral symmetry. Since the number of identical proteins in identical locations in a capsid exhibiting symmetry equals the order of the corresponding symmetry group, and since the icosahedral group is the finite group in three dimensions of largest order (order 60), this predominance of icosahedral symmetry in virus architecture is a logical consequence of sequence economy of the viral genome.

---

<sup>1</sup>E-mail: tk506@york.ac.uk

<sup>2</sup>E-mail: rt507@york.ac.uk

Icosahedral symmetry alone, however, cannot explain the surface structures of viral capsids with more than 60 capsid proteins. Therefore, Caspar and Klug introduced the concept of quasi-equivalence, which states that capsid proteins must be organised such that their local environments are almost equivalent. From a mathematical point of view, they realised this concept by classifying viral capsids in terms of triangulations with overall icosahedral symmetry. Their approach implies that viral capsids are organised in terms of clusters of capsid proteins, called capsomeres, and that viral capsids have precisely 12 clusters of five proteins (pentamers) and  $10(T - 1)$  clusters of six proteins (hexamers), where  $T$ , called the  $T$ -number, takes on any value  $k^2 + kn + n^2$  with  $k, n \in \mathbb{N}$  [2]. Caspar-Klug Theory has become a fundamental concept in virology with a plethora of applications, including the reconstruction of capsid shapes from experimental data and their classification.

However, experiments concerning the cancer-causing Papovaviridae have shown that there are viruses that do not follow the organisation predicted by Caspar-Klug Theory [3, 4]. These viruses have pentamers throughout (for example 72 pentamers in the case of Human Papilloma Virus), and their surface structures can hence not be described via triangulations. It has been shown in [5, 6, 7] that Caspar-Klug Theory can be generalised to incorporate these cases by considering not only lattice structures, but also quasi-lattices as known from the study of quasicrystals [8], i.e. alloys with atomic arrangements exhibiting long-range order but no periodicity [9]. However, a common feature of this approach and Caspar-Klug Theory is the fact that they use icosahedral symmetry as the maximal symmetry content in the theory and therefore describe viral capsids schematically in terms of surface lattices or tessellations, rather than as objects extended in space. As a consequence, the predictive power of these theories is limited to specifying the locations and types of the protein clusters in the capsids, their relative orientations, and, as in the case of the tiling approach, the locations of the bonds between the capsid proteins. But information on the tertiary structures of the capsid proteins, the thickness of the capsid and the organisation of the genomic material are inaccessible.

In this paper we address the question of whether there is more symmetry present in the organisation of viruses than presently appreciated. *It has been observed that the capsid proteins in different families of viruses may have similar tertiary structures even though their primary structures differ strongly, which led to the conjecture that these viruses have a common ancestor [24]. However, the similarity in their tertiary structures may be an implicit consequence of the limited number of structural blueprints available, i.e. may be due to a purely geometric constraint, and hence be a result of convergent evolution.* It is known – for example from the study of nested carbon cage structures called Carbon onions [10] – that the symmetry of an extended structure, that exhibits a certain compact symmetry such as icosahedral symmetry at different radial levels, can be described by an affine extension of this symmetry group. Analogous to this, we aim here at describing the full three-dimensional structures of viruses, i.e. the organisation of material at different radial levels collectively, in terms of affine extensions of the icosahedral group.

In order to be predictive, we classify all possible affine extensions of the icosahedral group that are relevant to simple viruses. For crystallographic groups, the classification of affine extensions has been considered before and corresponds to the derivation of space groups from point groups. In the non-crystallographic setting such as the case of the icosahedral group in three dimensions an equivalent approach does not apply because the symmetries described by such groups are not compatible with (periodic) lattices. Little is known about affine extensions of non-crystallographic groups. Previous approaches considering affine extensions

of the non-crystallographic Coxeter group  $H_3$  in the framework of quasicrystals [11] are relevant here because they contain the icosahedral group as a subgroup; however, the approach adopted in that reference is too restrictive in the context of viruses and only contains a subset of the structures we derive in this paper. In order to be comprehensive we introduce here the new mathematical concept of a *symmetry system* consisting of a symmetry group and a realisation of this group in terms of a set of vectors, called the *start configuration*. We show in Section 2 that the affine extensions of a symmetry group within a symmetry system depends on the start configuration. We classify affine extensions of symmetry systems based on the icosahedral group and a distinguished set of start configurations. We then show in Section 4 that these extended symmetry systems give rise to nested point configurations encoding their structures in a similar way as the vertex sets of the Platonic solids encode the structures of the compact symmetry groups in three dimensions via the action of the group generators on any member of the set. We classify all point sets that are associated with the extended symmetry systems in our classification, and show that there are 41 different such lattice-like point sets. In Section 5 we consider applications in virology and demonstrate that these lattice-like structures predict material boundaries in simple viruses. Based on the example of Pariacoto we explain how this approach implies predictions on the spatial extensions of the virus, including the tertiary structure of the capsid proteins and the organisation of the genomic material within the capsids. These results are complimentary to the predictions of Caspar-Klug Theory and apply to viruses of any  $T$ -number. We conclude by discussing the implications of our approach on virus assembly and viral evolution.

## 2 Symmetry systems and their affine extensions

Inspired by work of Janner [12, 13], we are seeking extensions of a non-crystallographic point group  $G$  by a (non-compact) translation operator  $T$  such that the monomials of the extended group, i.e products formed from the generators of  $G$  together with  $T$ , generate lattice-like point sets that are finite subsets of the aperiodic structures known from the study of quasicrystals. *An important property of these lattice-like point sets is that the symmetry of  $G$  is preserved throughout the points. That is, both the relative radial distribution of the points and the positions of the internal points are fixed by the symmetry of the group. Hence for a set of points with a specific external distribution of points, there is only one possible configuration for the internal points. Given a virus with external icosahedral symmetry, we have used lattice-like point sets generated by affine extensions of the icosahedral group to investigate the internal structures of viral capsids based on the external structure.*

Since the lattice-like point sets are generated by the actions of the monomials of the extended symmetry group on a vector  $v$ , the extensions of  $G$  leading to meaningful point-sets in the above sense depend on the choice of  $v$ . We therefore introduce the concept of a symmetry system.

**Definition 2.1** *For a symmetry group  $G$  and a vector  $v \in \mathbb{R}^k$ ,  $k \in \mathbb{N}$ , let  $\Delta(G, v)$  denote the set of vectors in  $\mathbb{R}^k$  generated by the action of  $G$  on  $v$ . Then we call the pair  $(G, v)$  the symmetry system associated with the start configuration  $\Delta(G, v)$ .*

Given a symmetry system  $(G, v)$  we are interested in extensions of  $G$  by a translation  $T$  such that the monomials in the generators of the extended group  $G^T$  that can be written in

terms of one occurrence of  $T$ , i.e. the products of the form  $gT$  with  $g \in G$  fulfil identities of the form  $m(g_1, T)v = m(g_2, T)v$ . Such identities ensure that the extended group has a non-trivial mathematical structure and that the point sets we are going to construct from them have minimal cardinality. We therefore introduce the following *monomial condition*:

**Definition 2.2** Let  $(G, v)$  be a symmetry system. We call a translation  $T$  with  $Tv = v + w$  an admissible translation if  $w$  is such that  $T$  is along a symmetry axis such that there are at least two points  $u_1, u_2 \in \Delta(G, v)$  with  $Tu_1$  and  $Tu_2$  situated on (different) symmetry axes of  $G$ . In this situation we call  $(G^T, v)$  the extended symmetry system associated with  $(G, v)$

Let moreover  $M^s(G, T)$  denote the set of monomials generated by any of the elements of  $G$  and precisely  $s$  copies of  $T$ . Then we say that two symmetry systems  $(G^{T_1}, v)$  and  $(G^{T_2}, v)$  are identical if  $M^s(G, T_1)v = M^s(G, T_2)v$  for all  $s \in \mathbb{N}$ ; otherwise, we call them distinct.

We demonstrate these concepts in Fig. 1 for the two-dimensional example of the cyclic group of order 5,  $C_5$ , that describes the rotational symmetries of a pentagon. Given a vector

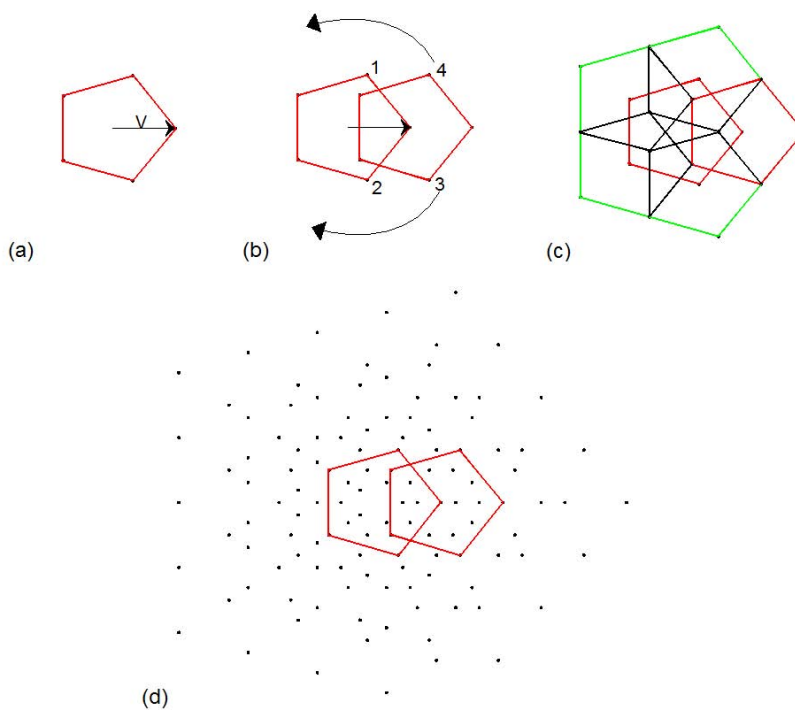


Figure 1: The monomial condition demonstrated for the cyclic group of order 5. (a-c) A translation by  $v$  combined with rotations produces lattice-like points. (d) Repeat applications produce denser and more spacially extended lattice-like point sets.

$v$  that points to one of the vertices of a pentagon, all other vertices are obtained via the action of the symmetry group  $C_5$ . In particular, with  $R$  denoting an anti-clockwise rotation by an angle  $\frac{2\pi}{5}$ , the vectors  $\vec{1}$  and  $\vec{2}$  corresponding, respectively, to the vertices labelled 1 and 2 in Fig. 1(b), can be expressed as  $\vec{1} = Rv$  and  $\vec{2} = R^4v$ . We are looking for extensions of the

symmetry system  $(C_5, v)$  by a translation such that the monomial condition is fulfilled. By definition, this is achieved by translations that lead to degeneracies among the monomials of the extended group, i.e. which are such that there exist different monomials that coincide when acting on  $v$ . Indeed, the vertex marked 4 in the figure can be obtained in different ways via the action of the extended symmetry group on  $v$ : via a translation of vertex 1 (corresponding to  $Rv$ ) by  $T$ , i.e.  $\vec{4} = TRv$ , or, by a translation of the vertex marked 2 (corresponding to  $R^4v$ ) on the one marked 3 followed by a rotation, i.e.  $\vec{4} = RTR^4v$ . A translation by  $v$  hence corresponds to an admissible translation according to Definition 2.2.

Some admissible translations are distinguished by the fact that they moreover fulfill the following *translation condition*:

**Definition 2.3** *Let  $(G, v)$  be a symmetry system with start configuration  $\Delta(G, v)$ . Then we say that  $T$  fulfills the translation condition provided that there exists  $w \in \Delta(G, v)$  such that  $Tw \in \Delta(G, v)$ .*

*If an admissible translation  $T$  for  $(G, v)$  fulfills the translation condition we call  $T$  a special translation for  $(G, v)$ .*

Note that the monomial and translation condition ensure an economy in the size of the point set generated by the action of the extended group  $G^T$  on  $v$  (such as the set in Fig. 1(d)). They hence distinguish extensions of  $G$  by an admissible or special translation from those by arbitrary translation operators.

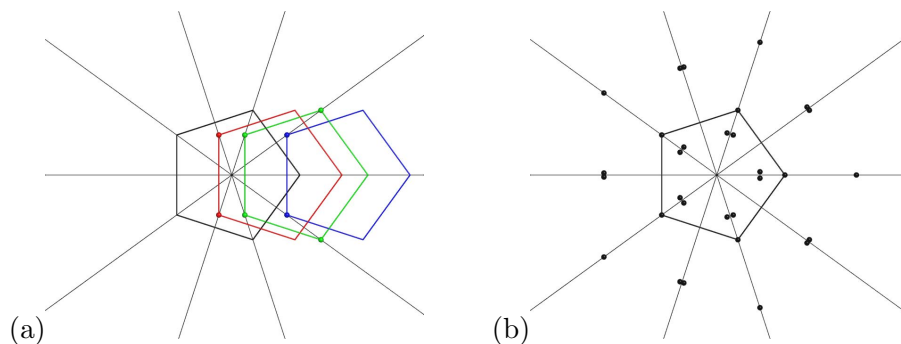


Figure 2: (a) Three admissible translations for the cyclic group of order 5. (b) A point set produced by a non-admissible translation.

We demonstrate the implications of admissibility in Fig. 2; the admissible translations in Fig. 2(a) are such that vertices obtained by translation are reproduced under the subsequent action of  $C_5$ . For a translation that is not admissible, every point leads to a new point via  $C_5$ , and accumulating points as in Fig. 2(b) can occur.

### 3 Extended symmetry systems based on the icosahedral group

Since we are interested in applications in virology, we consider the case of the icosahedral group  $I$  in detail. There are three start configurations that are distinguished by set economy.

These correspond to the sets with the smallest cardinalities among those invariant under the action of the icosahedral group, and are given by the vectors pointing to the vertices of an icosahedron, a dodecahedron or an icosidodecahedron, see Fig. 3. We denote the

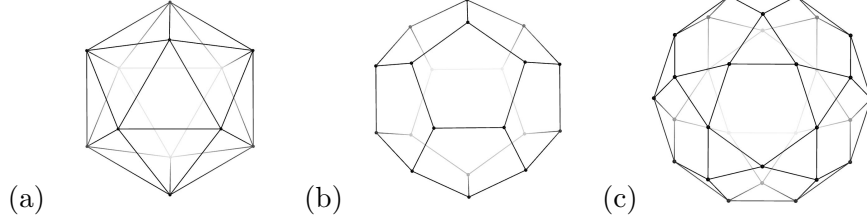


Figure 3: The icosahedron (a), dodecahedron (b) and icosidodecahedron (c) corresponding to the three distinguished start configurations  $\Delta(I, v_j)$ ,  $j = 1, 2, 3$ .

corresponding start configurations by  $\Delta(I, v_j)$ ,  $j = 1, 2, 3$ , with  $v_j$  pointing towards a vertex on a 5-, 3- or 2-fold axis of icosahedral symmetry, respectively.

Our strategy for determining all admissible translations for the symmetry systems  $(I, v_j)$ ,  $j = 1, \dots, 3$ , is hence as follows: In each case, we compute the admissible translations along the five-, three- and two-fold axes of icosahedral symmetry. We then determine which of these admissible translations are special translations in the sense of Definition 2.3. For future reference, we moreover list our results in a table at the end of each subsection.

### 3.1 The symmetry system $(I, v_1)$ with icosahedral start configuration

We express the 12 vectors in the icosahedral start configuration  $\Delta_1 := \Delta(I, v_1)$  by the following coordinates:

$$\Delta_1 = \{ (\pm 1, 0, \pm \tau) \quad \text{and all even permutations} \}, \quad (1)$$

where  $\tau := \frac{1}{2}(1 + \sqrt{5})$ . Since only translations along symmetry axes need to be considered, there are only three cases to consider.

*Case 1: Translations along a 5-fold axis.* Without loss of generality we consider translations along the vector  $\vec{T}_5 := (1, 0, \tau)$ . Since the admissible translations are characterised by the fact that they map vertices corresponding to vectors in  $\Delta(I, v_1)$  on symmetry axes. We therefore have to determine all translation lengths  $\lambda$  such that there exists  $u \in \Delta(I, v_1)$  with  $u + \lambda \vec{T}_5$  defining a point on an axis of icosahedral symmetry. In order to do so, we first decompose the set of vectors in  $\Delta(I, v_1)$  into maximal subsets invariant under a 5-fold rotation about  $\vec{T}_5$ :

$$\Delta(I, v_1) = \bigcup_{j=1}^2 V_j(T_5) \bigcup_{k=1}^2 V_k(T_5)^-, \quad (2)$$

where

$$\begin{aligned} V_1(T_5) &:= \{(1, 0, \tau)\} \\ V_2(T_5) &:= \{(\tau, -1, 0), (\tau, 1, 0), (0, \tau, 1), (-1, 0, \tau), (0, -\tau, 1)\} \end{aligned} \quad (3)$$

and  $V_1(T_5)^-$ ,  $V_2(T_5)^-$  the sets obtained from  $V_1(T_5)$  and  $V_2(T_5)$ , respectively, by inversion (i.e. by reversing the signs in front of all coordinates). For a graphical representation of these

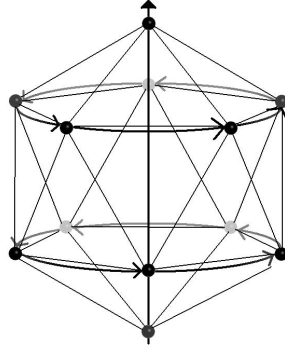


Figure 4: A graphical representation of the decomposition of the vertex set of the icosahedron under a rotation about  $T_5$ .

sets, see Fig. 4. Since vectors within the same subset lead to the same translation lengths  $\lambda$ , only a representative of each such subset needs to be considered. Moreover, the translation lengths of sets related by inversion can be inferred from each other: one obtains the same translation lengths but with a negative sign, i.e. translations in the opposite direction by the same lengths.

We start with the set  $V_2$  and without loss of generality choose  $\vec{v}_1 = (-\tau, 1, 0)$  as a representative. Fig. 5 shows a schematic representation of the locations of all symmetry axes that this vector might be mapped onto under a translation along  $\vec{T}_5$  (in positive or negative direction). To see how the two triangles in Fig. 5 relate to the faces of an icosahedron, compare

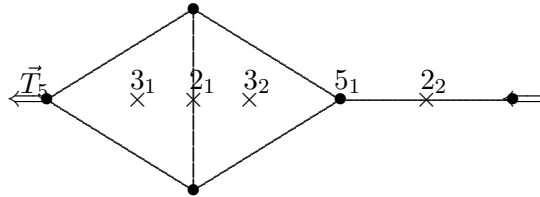


Figure 5: Schematic representation of the locations of the symmetry axes, denoted as  $2_1$ ,  $2_2$ ,  $3_1$ ,  $3_2$  and  $5$ , with respect to the translation direction given by  $\vec{T}_5$ .

with Fig. 6, which shows how the schematics relates to the surface of an icosahedron in a planar embedding. The locations of the 2- and 3-fold axes relative to the faces and edges of the icosahedron are also indicated in Fig. 5, and correspond to the following vectors (scaling chosen to match the coordinates used for the dodecahedron and icosidodecahedron in later subsections):

$$\begin{aligned} \vec{3}_1 &= (0, \tau', \tau) & \vec{2}_1 &= \frac{1}{2}(-1, \tau, \tau^2) & \vec{3}_2 &= (-1, 1, 1) \\ \vec{5}_1 &= (-\tau, 1, 0) & \vec{2}_2 &= \frac{1}{2}(-\tau^2, 1, -\tau). \end{aligned} \quad (4)$$

In order to determine the translation length  $\lambda^{3_1}$  such that the vertex located at  $5_1$  meets the axis denoted as  $3_1$  under a translation along  $\vec{T}_5$ , we need to solve the following equation for  $\lambda^{3_1}$  and  $\mu^{3_1} \in \mathbb{R}$ :

$$\vec{v}_1 + \lambda^{3_1} \vec{T}_5 = \mu^{3_1} \vec{3}_1. \quad (5)$$

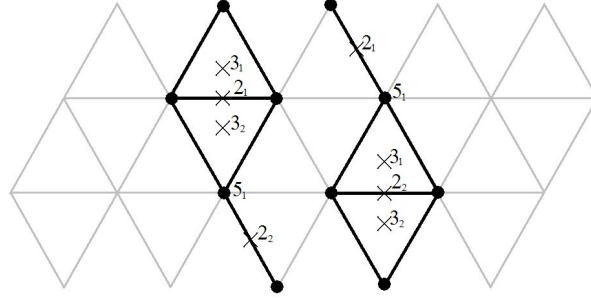


Figure 6: An icosahedral net with the two (equivalent) point sets for five-fold translation.

We obtain the solution  $\lambda^{3_1} = 1$ , and hence an admissible translation  $T = \lambda^{3_1} \vec{T}_5 = (1, 0, \tau)$ . Along similar lines, we solve the equations for  $2_1$ ,  $3_2$  and  $2_2$  resulting in the admissible translations  $T = -\tau' \vec{T}_5$ ,  $\vec{T}_5$  and  $\tau \vec{T}_5$ . Due to the symmetry of  $\Delta(I, v_1)$  translations of positive or negative sign lead to the same extended symmetry systems and it is hence sufficient to consider only the positive vectors when enumerating admissible translations corresponding to different extended symmetry systems.

Finally, we consider a representative of the set  $V_1(T_5)$  in (2). A translation of length 2 maps  $(-1, 0, -\tau)$  on  $(1, 0, \tau)$ . However, such a translation only fulfills the translation condition, but not the monomial condition, so it does not correspond to an admissible translation.

*Case 2: Translations along a 3-fold axis.* Without loss of generality we choose the translation direction  $\vec{T}_3 := (0, \tau', \tau)$ . Under a three-fold rotation about this translation axis, the vectors in  $\Delta(I, v_1)$  decompose into four sets of three as follows:

$$\Delta(I, v_1) = \bigcup_{j=1}^2 V_j(T_3) \bigcup_{k=1}^2 V_k(T_3)^-, \quad (6)$$

where

$$\begin{aligned} V_1(T_3) &:= \{(0, -\tau, 1), (-1, 0, \tau), (1, 0, \tau)\} \\ V_2(T_3) &:= \{(-\tau, -1, 0), (\tau, -1, 0), (0, \tau, 1)\} \end{aligned} \quad (7)$$

and  $V_1(T_3)^-$ ,  $V_2(T_3)^-$  the sets obtained from  $V_1(T_3)$  and  $V_2(T_3)$ , respectively, by inversion.

We hence only need to consider representatives of  $V_1(T_3)$  and  $V_2(T_3)$  explicitly. We encode the locations of representatives of these sets, denoted as  $5_1$  and  $5_2$ , and the locations of all symmetry axes these vertices can be mapped on by a translation along  $\vec{T}_3$  in the schematics in Fig. 7.

With

$$\begin{aligned} \vec{5}_1 &= (0, -\tau, 1) & \vec{2}_1 &= (0, -\tau, 0) & \vec{5}_2 &= (0, -\tau, -1) \\ \vec{3}_1 &= (0, \tau', -\tau) & \vec{2}_2 &= (0, 0, -\tau) \end{aligned} \quad (8)$$

we obtain the following translation lengths for  $\vec{5}_1$ :  $\lambda^{2_1} = \tau'$ ,  $\lambda^{5_2} = -1$ ,  $\lambda^{3_1} = -\tau$  and  $\lambda^{2_2} = -\tau^2$ . For  $\vec{5}_2$ , we obtain translations of the same absolute lengths but in opposite direction. Due to symmetry of  $\Delta(I, v_1)$  only admissible translations in one translation direction need to

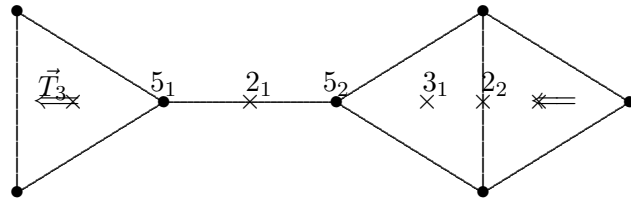


Figure 7: Schematic representation of the locations of the symmetry axes, denoted as  $2_1$ ,  $2_2$ ,  $3_1$ ,  $5_1$  and  $5_2$ , with respect to the translation direction given by  $\vec{T}_3$ .

be considered when enumerating distinct extended symmetry systems, and we hence obtain distinct extended symmetry systems for the following admissible translations along  $\vec{T}_3$ :  $T = -\tau'\vec{T}_3, \vec{T}_3, \tau\vec{T}_3, \tau^2\vec{T}_3$ . There are no translations in the direction of  $\vec{T}_3$  fulfilling the translation condition, so there are no special translations along this direction.

*Case 3: Translations along a 2-fold axis.* Without loss of generality we choose the translation direction  $\vec{T}_2 := (\tau, 0, 0)$ . With respect to a two-fold rotation along this axis, the 12 vertices decompose into four sets of two and one set of four as follows:

$$\Delta(I, v_1) = \bigcup_{j=1}^3 V_j(T_2) \bigcup_{k=1}^2 V_k(T_2)^-, \quad (9)$$

where

$$\begin{aligned} V_1(T_2) &:= \{(\tau, -1, 0), (\tau, 1, 0)\} \\ V_2(T_2) &:= \{(1, 0, -\tau), (1, 0, \tau)\} \\ V_3(T_2) &:= \{(0, -\tau, -1), (0, \tau, -1), (0, -\tau, 1), (0, \tau, 1)\} \end{aligned} \quad (10)$$

and  $V_1(T_2)^-, V_2(T_2)^-$  the sets obtained from  $V_1(T_2)$  and  $V_2(T_2)$ , respectively, by inversion. Since elements in  $V_3(T_2)$  can never be translated on a symmetry axis under a translation along the translation direction, only representatives of the sets  $V_1(T_2)$  and  $V_2(T_2)$  need to be considered.

We start with the set  $V_1(T_2)$ : As a representative of this set we use  $5_1$  in Fig. 8, and

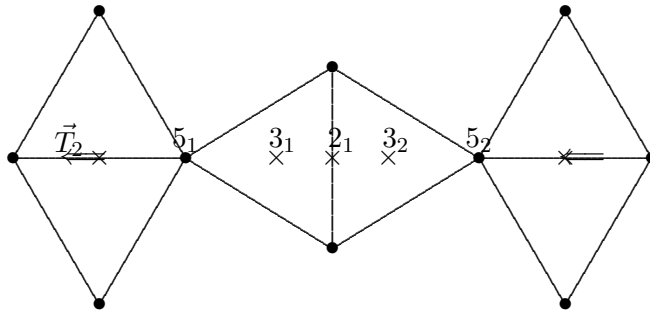


Figure 8: Schematic representation of the locations of the symmetry axes, denoted as  $2_1$ ,  $3_1$ ,  $3_2$ ,  $5_1$  and  $5_2$ , with respect to the translation direction given by  $\vec{T}_2$  for a representative of the set  $V_1(T_2)$ .

without loss of generality represent the symmetry axes by the following vectors:

$$\begin{aligned}\vec{5}_1 &= (\tau, -1, 0) & \vec{3}_1 &= (-\tau', -\tau, 0) & \vec{2}_1 &= (0, -\tau, 0) \\ \vec{3}_2 &= (\tau', -\tau, 0) & \vec{5}_2 &= (-\tau, -1, 0).\end{aligned}\tag{11}$$

We obtain the following translation lengths:  $\lambda^{3_1} = -2\tau'^2$ ,  $\lambda^{2_1} = -1$ ,  $\lambda^{3_2} = 2\tau'$  and  $\lambda^{5_2} = -2$ .

We next consider  $V_2(T_2)$  represented by  $5_1$  in Fig. 9. With

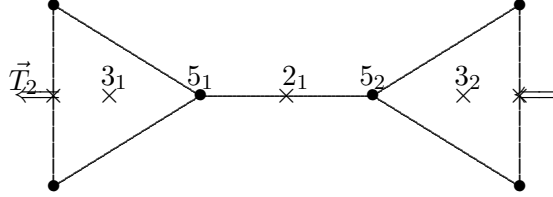


Figure 9: Schematic representation of the locations of the symmetry axes, denoted as  $2_1$ ,  $3_1$ ,  $3_2$ ,  $5_1$  and  $5_2$ , with respect to the translation direction given by  $\vec{T}_2$  for a representative of the set  $V_2(T_2)$ .

$$\begin{aligned}\vec{3}_1 &= (\tau, 0, \tau') & \vec{5}_1 &= (1, 0, -\tau) & \vec{2}_1 &= (0, 0, -\tau) \\ \vec{3}_2 &= (-1, 0, -\tau) & \vec{3}_2 &= (-\tau, 0, \tau')\end{aligned}\tag{12}$$

we obtain the following translation lengths:  $\lambda^{3_1} = 2$ ,  $\lambda^{2_1} = \tau'$ ,  $\lambda^{5_2} = 2\tau'$  and  $\lambda^{3_2} = -2\tau$ . In summary we obtain the following admissible translations in the direction  $\vec{T}_2$ :  $T = -\tau'\vec{T}_2$ ,  $2\tau'^2\vec{T}_2$ ,  $\vec{T}_2$ ,  $-2\tau'\vec{T}_2$ ,  $2\vec{T}_2$  and  $2\tau\vec{T}_2$ .

In order to see which of these are special translations we check the translation condition. In both cases, i.e. both in Fig. 8 and in Fig. 9, the only translations fulfilling the translation condition are those that map  $5_2$  on  $5_1$  via a translation of lengths  $2\vec{T}_2$ , or  $2\tau'\vec{T}_2$  respectively. These two translations are hence the only special translations.

This exhausts all admissible and special translations corresponding to distinct extended symmetry systems in the icosahedral case. We summarise the results in the following table:

Direction	admissible	special
$\vec{T}_5 = (1, 0, \tau)$	$-\tau'\vec{T}_5, \vec{T}_5, \tau\vec{T}_5$	
$\vec{T}_3 = (0, \tau', \tau)$	$-\tau'\vec{T}_3, \vec{T}_3, \tau\vec{T}_3, \tau^2\vec{T}_3$	
$\vec{T}_2 = (\tau, 0, 0)$	$-\tau'\vec{T}_2, \vec{T}_2, 2\tau\vec{T}_2, 2\tau'^2\vec{T}_2$	$-2\tau'\vec{T}_2, 2\vec{T}_2$

Table 1: *The admissible and special translations corresponding to distinct extended symmetry systems for the symmetry system  $(I, v_1)$ .*

### 3.2 The symmetry system $(I, v_2)$ with dodecahedral start configuration

We express the 20 vectors in the dodecahedral start configuration  $\Delta(I, v_2)$  by the following coordinates:

$$\Delta_2 = \left\{ \begin{array}{ll} (\pm 1, \pm 1, \pm 1) & \text{and all permutations} \\ (0, \pm \tau', \pm \tau) & \text{and all even permutations} \end{array} \right\}, \quad (13)$$

where  $\tau' := \frac{1}{2}(1 - \sqrt{5})$  and  $\tau$  as in (1). As before, we consider translations along the 5-, 3- and 2-fold axes of icosahedral symmetry separately.

*Case 1: Translations along a 5-fold axis.* We again consider the translation direction  $\vec{T}_5 = (1, 0, \tau)$ . The twenty vertices of the dodecahedron decompose into four sets of five under a rotation about this 5-fold axis as follows:

$$\Delta(I, v_2) = \bigcup_{j=1}^2 V_j(T_5) \bigcup_{k=1}^2 V_k(T_5)^-, \quad (14)$$

where

$$\begin{aligned} V_1(T_5) &:= \{(0, -\tau', \tau), (0, \tau', \tau), (\tau, 0, -\tau'), (1, -1, 1), (1, 1, 1)\} \\ V_2(T_5) &:= \{(-\tau', \tau, 0), (-\tau', -\tau, 0), (\tau, 0, -\tau'), (-1, -1, 1), (-1, 1, 1)\} \end{aligned} \quad (15)$$

and  $V_1(T_5)^-, V_2(T_5)^-$  the sets obtained from  $V_1(T_5)$  and  $V_2(T_5)$ , respectively, by inversion.

We chose the representatives  $3_1$  and  $3_2$  for the sets  $V_1(T_5)$  and  $V_2(T_5)$ , and indicate their locations as well as those of the axes they might be translated to, schematically in Fig. 10.

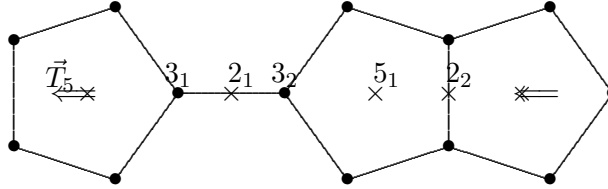


Figure 10: Schematic representation of the locations of the symmetry axes, denoted as  $2_1$ ,  $2_2$ ,  $3_1$ ,  $3_2$  and  $5_1$ , with respect to the translation direction given by  $\vec{T}_5$  for representatives of the sets  $V_1(T_5)$  and  $V_2(T_5)$ .

With

$$\begin{aligned} \vec{3}_1 &= (0, -\tau', \tau) & \vec{2}_1 &= \frac{1}{2}(-1, \tau, \tau^2) & \vec{3}_2 &= (-1, 1, 1) \\ \vec{5}_1 &= (-\tau, 1, 0) & \vec{2}_2 &= \frac{1}{2}(-\tau^2, 1, -\tau) \end{aligned} \quad (16)$$

we obtain the following admissible translations for  $3_1$ :  $\lambda^{2_1} = -\tau'^2$ ,  $\lambda^{3_2} = \tau'$ ,  $\lambda^{5_1} = -1$  and  $\lambda^{2_2} = -\tau$ . For the vector corresponding to  $3_2$ , we obtain translations of the same lengths but in opposite directions.

In summary, the admissible translations leading to distinct extended symmetry systems with direction  $\vec{T}_5$  are:  $T = \tau'^2 \vec{T}_5$ ,  $-\tau' \vec{T}_5$ ,  $\vec{T}_5$  and  $\tau \vec{T}_5$ , and there are no special translations along this direction.

*Case 2: Translations along a 3-fold axis.* Without loss of generality we choose the vector  $\vec{T}_3 := (0, \tau', \tau)$  as translation direction. Under the action of a 3-fold rotation about this vector

$\Delta(I, v_2)$  decomposes into two sets of one vertex each located on the translation direction, two sets of three, and two sets of six as follows:

$$\Delta(I, v_2) = \bigcup_{j=1}^3 V_j(T_3) \bigcup_{k=1}^3 V_k(T_3)^-, \quad (17)$$

where

$$\begin{aligned} V_1(T_3) &:= \{(0, \tau', \tau)\} \\ V_2(T_3) &:= \{(0, -\tau', \tau), (-1, -1, 1), (1, -1, 1)\} \\ V_3(T_3) &:= \{(-\tau', -\tau, 0), (\tau', -\tau, 0), (\tau, 0, -\tau'), (-\tau, 0, -\tau'), (-1, 1, 1), (1, 1, 1)\} \end{aligned} \quad (18)$$

and  $V_1(T_3)^-, V_2(T_3)^-, V_3(T_3)^-$  the sets obtained from  $V_1(T_3), V_2(T_3)$  and  $V_3(T_3)$ , respectively, by inversion.

Since the elements of  $V_3(T_3)$  cannot be translated onto any of the symmetry axes under a translation along a three-fold axis, only the sets  $V_1(T_3)$  and  $V_2(T_3)$  have to be considered explicitly. For  $V_1(T_3)^-$  and  $V_2(T_3)^-$  the same translation lengths but opposite translation directions are automatically obtained due to inversion symmetry. For the element in  $V_1(T_3)$  there exists a translation that fulfils the translation condition but not the monomial condition and hence does not correspond to an admissible translation.

We schematically encode a representative of  $V_2(T_3)$ ,  $3_1$ , together with the locations of all symmetry axes it may be translated onto in Fig. 11.

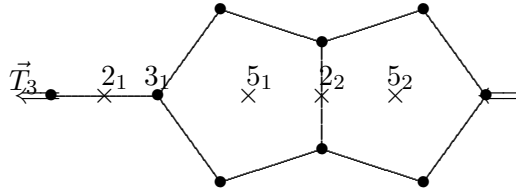


Figure 11: Schematic representation of the locations of the symmetry axes, denoted as  $2_1, 2_2, 3_1, 5_1$  and  $5_2$ , with respect to the translation direction given by  $\vec{T}_3$  for a representative of the set  $V_2(T_3)$ .

With

$$\begin{aligned} \vec{2}_1 &= (0, 0, 1) & \vec{3}_1 &= (0, -\tau', \tau) & \vec{5}_1 &= (0, \tau, 1) \\ \vec{2}_2 &= (0, 1, 0) & \vec{5}_2 &= (0, \tau, -1) \end{aligned} \quad (19)$$

we obtain the following translation lengths:  $\lambda^{2_1} = 1, \lambda^{5_1} = \tau', \lambda^{2_2} = -1$  and  $\lambda^{5_2} = -\tau$ . Due to symmetry of the start configuration, the following admissible translations with direction  $\vec{T}_3$  correspond to different extended symmetry systems:  $T = -\tau'\vec{T}_3, \vec{T}_3$  and  $\tau\vec{T}_3$ . There are no special translations, because translations fulfilling the translation condition do not fulfill the monomial condition.

*Case 3: Translations along a two-fold axis.* Without loss of generality we again choose the translation direction to be  $\vec{T}_2 := (\tau, 0, 0)$ . Under the action of a two-fold rotation about this vector,  $\Delta(I, v_2)$  decomposes into three sets of four vertices and four sets of two vertices

as follows:

$$\Delta(I, v_2) = \bigcup_{j=1}^4 V_j(T_2) \bigcup_{k=1}^3 V_k(T_2)^-, \quad (20)$$

where

$$\begin{aligned} V_1(T_2) &:= \{(\tau, 0, -\tau'), (\tau, 0, \tau')\} \\ V_2(T_2) &:= \{(1, -1, -1), (1, 1, -1), (1, -1, 1), (1, 1, 1)\} \\ V_3(T_2) &:= \{(-\tau', \tau, 0), (-\tau', -\tau, 0)\} \\ V_4(T_2) &:= \{(0, \tau', \tau), (0, -\tau', \tau), (0, \tau', -\tau), (0, -\tau', -\tau)\} \end{aligned} \quad (21)$$

and  $V_1(T_2)^-$ ,  $V_2(T_2)^-$  and  $V_3(T_2)^-$  the sets obtained from  $V_1(T_2)$ ,  $V_2(T_2)$  and  $V_3(T_2)$ , respectively, by inversion. Since the vertices in  $V_4(T_2)$  can not be translated onto symmetry axes, only representatives of the sets  $V_1(T_2)$ ,  $V_2(T_2)$  and  $V_3(T_2)$  need to be considered.

We represent  $V_1(T_2)$  by  $3_1$  in Fig. 12, with symmetry axes given by the vectors in (22).

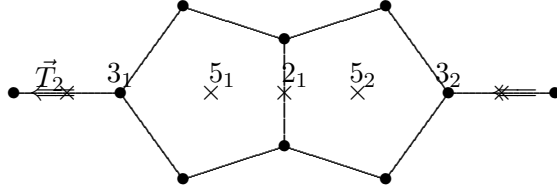


Figure 12: Schematic representation of the locations of the symmetry axes, denoted as  $2_1$ ,  $3_1$ ,  $3_2$ ,  $5_1$  and  $5_2$ , with respect to the translation direction given by  $\vec{T}_2$  for a representative of the set  $V_1(T_2)$ .

$$\begin{aligned} \vec{3}_1 &= (\tau, 0, -\tau') & \vec{5}_1 &= (1, 0, \tau) & \vec{2}_1 &= (0, 0, \tau) \\ \vec{5}_2 &= (-1, 0, \tau) & \vec{3}_2 &= (-\tau, 0, -\tau'). \end{aligned} \quad (22)$$

The vertex  $3_1$  can be translated on these symmetry axes under translations of the following lengths:  $\lambda^{5_1} = -2\tau'^2$ ,  $\lambda^{2_1} = -1$ ,  $\lambda^{5_2} = 2\tau'$  and  $\lambda^{3_2} = -2$ , and translations of opposite direction are obtained for the set related by inversion (represented by  $3_2$ ).

For  $V_2(T_2)$  we obtain the scenario represented by  $3_1$  in Fig. 13.

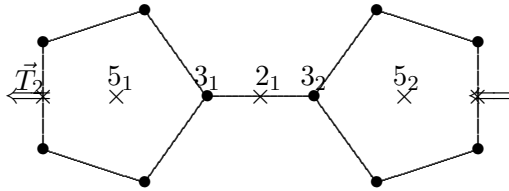


Figure 13: Schematic representation of the locations of the symmetry axes, denoted as  $2_1$ ,  $3_1$ ,  $3_2$ ,  $5_1$  and  $5_2$ , with respect to the translation direction given by  $\vec{T}_2$  for a representative of the set  $V_2(T_2)$ .

With

$$\begin{aligned} \vec{5}_1 &= (\tau, -1, 0) & \vec{3}_1 &= (-\tau', -\tau, 0) & \vec{2}_1 &= (0, -\tau, 0) \\ \vec{5}_2 &= (\tau', -\tau, 0) & \vec{5}_2 &= (-\tau, -1, 0) \end{aligned} \quad (23)$$

$3_1$  can be translated on these symmetry axes under translations of the following lengths:  $\lambda^{5_1} = -2\tau'$ ,  $\lambda^{2_1} = -\tau'^2$ ,  $\lambda^{3_2} = -2\tau'^2$  and  $\lambda^{5_2} = -2$ .

In summary, the following admissible translations correspond to all distinct extended symmetry systems along  $\vec{T}_2$ :  $T = \tau'^2\vec{T}_2$ ,  $2\tau'^2\vec{T}_2$ ,  $\vec{T}_2$ ,  $-2\tau'\vec{T}_2$  and  $2\vec{T}_2$ . Among these  $T = 2\tau'^2\vec{T}_2$ ,  $2\tau'\vec{T}_2$  and  $2\vec{T}_2$  are special translations because they also fulfill the translation condition.

We summarise the results for the dodecahedral case in the following table:

Direction	admissible	special
$\vec{T}_5 = (1, 0, \tau)$	$\tau'^2\vec{T}_5, -\tau'\vec{T}_5, \vec{T}_5, \tau\vec{T}_5$	
$\vec{T}_3 = (0, \tau', \tau)$	$-\tau'\vec{T}_3, \vec{T}_3, \tau\vec{T}_3$	
$\vec{T}_2 = (\tau, 0, 0)$	$\tau'^2\vec{T}_2, \vec{T}_2$	$2\tau'^2\vec{T}_2, -2\tau'\vec{T}_2, 2\vec{T}_2$

Table 2: *Admissible and special translations leading to distinct extended symmetry systems for  $(I, v_2)$ .*

### 3.3 The symmetry system $(I, v_3)$ with icosidodecahedral start configuration

We represent the 30 vectors in  $\Delta(I, v_3)$  by

$$\Delta_3 = \left\{ \begin{array}{ll} (\pm\tau, 0, 0) & \text{and all permutations} \\ \frac{1}{2}(\pm 1, \pm\tau, \pm\tau^2) & \text{and all even permutations} \end{array} \right\}, \quad (24)$$

where  $\tau$  is given by (1). As before we need to consider translations along a 5-, 3- and 2-fold axis of icosahedral symmetry separately.

*Case 1: Translations along a 5-fold axis.* Without loss of generality we again choose  $\vec{T}_5 = (1, 0, \tau)$  as translation direction. Under a rotation about  $\vec{T}_5$  the set of vertices decomposes into four sets of five and one set of ten as follows:

$$\Delta(I, v_3) = \bigcup_{j=1}^3 V_j(T_5) \bigcup_{k=1}^2 V_k(T_5)^-, \quad (25)$$

where

$$\begin{aligned} V_1(T_5) &:= \{(0, 0, \tau), \frac{1}{2}(\tau^2, -1, \tau), \frac{1}{2}(\tau^2, 1, \tau), \frac{1}{2}(1, \tau, \tau^2), \frac{1}{2}(1, -\tau, \tau^2)\} \\ V_2(T_5) &:= \{(\tau, 0, 0), \frac{1}{2}(\tau, \tau^2, 1), \frac{1}{2}(\tau, -\tau^2, 1), \frac{1}{2}(-1, \tau, \tau^2), \frac{1}{2}(-1, -\tau, \tau^2)\} \\ V_3(T_5) &:= \{(0, \tau, 0), (0, -\tau, 0), \frac{1}{2}(-\tau^2, -1, \tau), \frac{1}{2}(\tau^2, -1, -\tau), \frac{1}{2}(-\tau^2, 1, \tau), \\ &\quad \frac{1}{2}(\tau^2, 1, -\tau), \frac{1}{2}(\tau, \tau^2, -1), \frac{1}{2}(\tau, -\tau^2, -1), \frac{1}{2}(-\tau, \tau^2, 1), \frac{1}{2}(-\tau, -\tau^2, 1)\} \end{aligned} \quad (26)$$

and  $V_1(T_5)^-$ ,  $V_2(T_5)^-$  the sets obtained from  $V_1(T_5)$  and  $V_2(T_5)$ , respectively, by inversion. Vertices in  $V_3(T_5)$  can not be translated on any of the symmetry axes, and we therefore only need to compute the admissible translations for representative vertices of  $V_1(T_5)$  and  $V_2(T_5)$ . We represent these vertices, denoted as  $2_1$  and  $2_2$ , in the schematics in Fig. 14, and use the following coordinate representations for the symmetry axes:

$$\begin{aligned} \vec{2}_1 &= (0, 0, \tau) & \vec{5}_1 &= (-1, 0, \tau) & \vec{3}_1 &= (-\tau, 0, -\tau') \\ \vec{2}_2 &= (-\tau, 0, 0) & \vec{3}_2 &= (-\tau, 0, \tau'). \end{aligned} \quad (27)$$

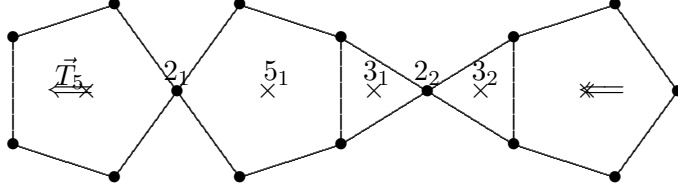


Figure 14: Schematic representation of the locations of the symmetry axes, denoted as  $2_1$ ,  $2_2$ ,  $3_1$ ,  $3_2$  and  $5_1$ , with respect to the translation direction given by  $\vec{T}_5$  for representatives of the sets  $V_1(T_5)$  and  $V_2(T_5)$ .

Vertex  $2_1$  can be translated on these symmetry axes with translations of the following lengths:  $\lambda^{5_1} = -1/2$ ,  $\lambda^{3_1} = -\tau/2$ ,  $\lambda^{2_2} = -1$  and  $\lambda^{3_2} = -\tau^2/2$ . For the vertex  $2_2$  we moreover obtain the solutions  $\lambda^{2_1} = \tau$ ,  $\lambda^{5_1} = \tau/2$ ,  $\lambda^{3_1} = -\tau'/2$  and  $\lambda^{3_2} = -1/2$ . Furthermore, also the negative translation lengths occur for the other sets of vertices that are related to these cases by inversion. However, they lead to the same extended symmetry systems due to the symmetry of the start configuration and therefore do not need to be considered here.

In summary, we obtain the following admissible translations in the direction  $\vec{T}_5$  leading to different extended symmetry systems:  $T = -\frac{1}{2}\tau'\vec{T}_5$ ,  $\frac{1}{2}\vec{T}_5$ ,  $\frac{1}{2}\tau\vec{T}_5$ ,  $\vec{T}_5$ ,  $\frac{1}{2}\tau^2\vec{T}_5$  and  $\tau\vec{T}_5$ . None of these are special translations.

*Case 2: Translations along a three-fold axis.* Without loss of generality we again use the translation direction  $\vec{T}_3 := (0, \tau', \tau)$ . Under a rotation about this axis, the vertex set decomposes into three sets of six vertices and four sets of three as follows:

$$\Delta(I, v_3) = \bigcup_{j=1}^4 V_j(T_2) \bigcup_{k=1}^3 V_k(T_2)^-, \quad (28)$$

where

$$\begin{aligned} V_1(T_3) &:= \{(0, 0, \tau), \frac{1}{2}(-1, -\tau, \tau^2), \frac{1}{2}(1, -\tau, \tau^2)\} \\ V_2(T_3) &:= \{\frac{1}{2}(\tau^2, -1, \tau), \frac{1}{2}(-\tau^2, -1, \tau), \frac{1}{2}(\tau, -\tau^2, 1), \frac{1}{2}(-\tau, -\tau^2, 1), \frac{1}{2}(-1, \tau, \tau^2), \frac{1}{2}(1, \tau, \tau^2)\} \\ V_3(T_3) &:= \{(0, -\tau, 0), \frac{1}{2}(\tau^2, 1, \tau), \frac{1}{2}(-\tau^2, 1, \tau)\} \\ V_4(T_3) &:= \{(\tau, 0, 0), (-\tau, 0, 0), \frac{1}{2}(\tau, -\tau^2, -1), \frac{1}{2}(\tau, \tau^2, 1), \frac{1}{2}(-\tau, -\tau^2, -1), \frac{1}{2}(-\tau, \tau^2, 1)\} \end{aligned} \quad (29)$$

and  $V_1(T_3)^-$ ,  $V_2(T_3)^-$  and  $V_3(T_3)^-$  the sets obtained from  $V_1(T_3)$ ,  $V_2(T_3)$  and  $V_3(T_3)$ , respectively, by inversion. Elements of  $V_2(T_3)$  and  $V_4(T_3)$ , and the corresponding sets obtained by inversion, can not be translated on any of the symmetry axes and hence do not need to be considered. Representatives of the sets  $V_1(T_3)$  and  $V_3(T_3)$  are shown as  $2_1$  and  $2_2$  in the schematics in Fig. 15.

With

$$\begin{aligned} \vec{2}_1 &= (0, 0, \tau) \\ \vec{3}_1 &= (0, -\tau', \tau) & \vec{5}_1 &= (0, \tau, 1) & \vec{2}_2 &= (0, \tau, 0) \\ \vec{5}_2 &= (0, \tau, -1) \end{aligned} \quad (30)$$

we find the following translation lengths for  $2_1$ :  $\lambda^{3_1} = -1/2$ ,  $\lambda^{5_1} = -\tau/2$ ,  $\lambda^{2_2} = -1$  and  $\lambda^{5_2} = -\tau^2/2$ . Moreover, for the vertex  $2_2$  we obtain  $\lambda^{2_1} = \tau^2$ ,  $\lambda^{3_1} = \tau^2/2$ ,  $\lambda^{5_1} = 1/2$  and

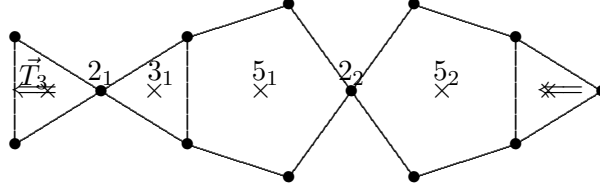


Figure 15: Schematic representation of the locations of the symmetry axes, denoted as  $2_1$ ,  $2_2$ ,  $3_1$ ,  $5_1$  and  $5_2$ , with respect to the translation direction given by  $\vec{T}_3$  for representatives of the sets  $V_1(T_3)$  and  $V_3(T_3)$ .

$\lambda^{5_2} = -\tau/2$ . As before, translations in opposite direction are obtained for the sets related by inversion.

In summary, the following admissible translations in the direction  $\vec{T}_3$  correspond to distinct extended symmetry systems:  $T = \frac{1}{2}\vec{T}_3, \frac{1}{2}\tau\vec{T}_3, \vec{T}_3, \frac{1}{2}\tau^2\vec{T}_3$  and  $\tau^2\vec{T}_3$ .

*Case 3: Translations along a 2-fold symmetry axis.* Under a rotation about the two-fold symmetry axis  $\vec{T}_2 := (\tau, 0, 0)$ ,  $\Delta(I, v_3)$  decomposes into two sets of one, two sets of two and six sets of four as follows:

$$\Delta(I, v_3) = \bigcup_{j=1}^6 V_j(T_2) \bigcup_{k=1}^4 V_k(T_2)^-, \quad (31)$$

where

$$\begin{aligned} V_1(T_2) &:= \{(\tau, 0, 0)\} \\ V_2(T_2) &:= \{\frac{1}{2}(\tau^2, -1, \tau), \frac{1}{2}(\tau^2, 1, \tau), \frac{1}{2}(\tau^2, -1, -\tau), \frac{1}{2}(\tau^2, 1, -\tau)\} \\ V_3(T_2) &:= \{\frac{1}{2}(\tau, \tau^2, -1), \frac{1}{2}(\tau, -\tau^2, -1), \frac{1}{2}(\tau, \tau^2, 1), \frac{1}{2}(\tau, -\tau^2, 1)\} \\ V_4(T_2) &:= \{\frac{1}{2}(1, \tau, \tau^2), \frac{1}{2}(1, -\tau, \tau^2), \frac{1}{2}(1, \tau, -\tau^2), \frac{1}{2}(1, -\tau, -\tau^2)\} \\ V_5(T_2) &:= \{(0, \tau, 0), (0, -\tau, 0)\} \\ V_6(T_2) &:= \{(0, 0, \tau), (0, 0, -\tau)\} \end{aligned} \quad (32)$$

and  $V_1(T_2)^-, V_2(T_2)^-, V_3(T_2)^-$  and  $V_4(T_2)^-$  the sets obtained from  $V_1(T_2), V_2(T_2), V_3(T_2)$  and  $V_4(T_2)$ , respectively, by inversion. Elements of  $V_3(T_2)$  and its inverse set can not be translated on any of the symmetry axes and hence do not need to be considered explicitly. For  $V_1^-(T_2)$  one obtains a translation,  $2\vec{T}_2$ , that fulfils the translation condition, but does not abide to the monomial condition.

Hence, only representatives of the sets  $V_2(T_2), V_4(T_2)$  and  $V_5(T_2)$  need to be considered explicitly, and we show their locations in three different schematics below.

We start by considering the set  $V_5(T_2)$  represented by  $2_1$  in the schematics in Fig. 16. Note that translations onto the axes labelled  $5_2$  and  $3_2$  do not need to be considered explicitly because the corresponding translations are of the same lengths (but in opposite direction) as those for  $3_1$  and  $5_1$  by symmetry.

With the following expression for the symmetry axes,

$$\begin{aligned} \vec{5}_1 &= (\tau, -1, 0) \\ \vec{3}_1 &= (-\tau', -\tau, 0) \quad \vec{2}_1 = (0, -\tau, 0), \end{aligned} \quad (33)$$

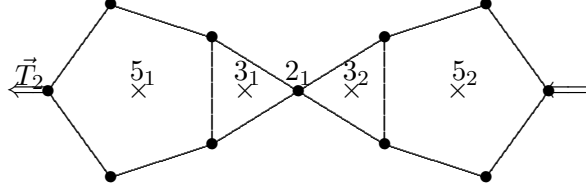


Figure 16: Schematic representation of the locations of the symmetry axes, denoted as  $2_1$ ,  $3_1$ ,  $3_2$ ,  $5_1$  and  $5_2$ , with respect to the translation direction given by  $\vec{T}_2$  for representatives of the set  $V_5(T_2)$ .

we obtain the translation lengths  $\lambda^{5_1} = \tau$  and  $\lambda^{3_1} = \tau'^2$ .

As a representative of  $V_6(T_2)$  we consider  $2_1$  in Fig. 17. As before, only translations on axes labelled  $3_1$  and  $5_1$  need to be considered as results for  $5_2$  and  $3_2$  follow by symmetry.

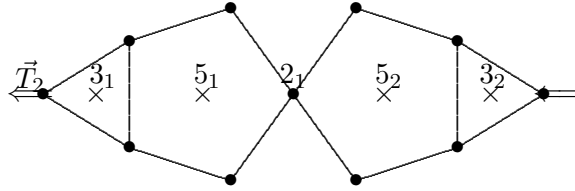


Figure 17: Schematic representation of the locations of the symmetry axes, denoted as  $2_1$ ,  $3_1$ ,  $3_2$ ,  $5_1$  and  $5_2$ , with respect to the translation direction given by  $\vec{T}_2$  for representatives of the set  $V_6(T_2)$ .

With

$$\vec{3}_1 = (\tau, 0, -\tau') \quad \vec{5}_1 = (1, 0, \tau) \quad \vec{2}_1 = (0, 0, \tau) \quad (34)$$

we obtain the translation lengths  $\lambda^{3_1} = \tau^2$  and  $\lambda^{5_1} = -\tau'$ .

Finally, the sets  $V_2(T_2)$  and  $V_4(T_2)$  are represented by Fig. 18 and we consider translations of their representatives  $2_1$  and  $2_2$ .

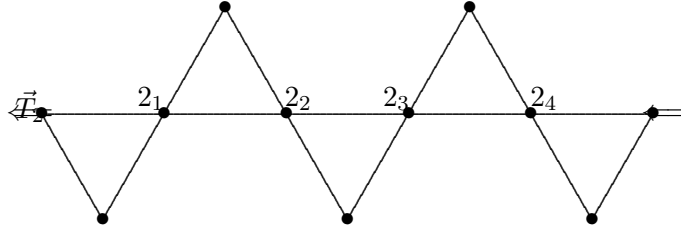


Figure 18: Schematic representation of the locations of the symmetry axes, denoted as  $2_1$ ,  $2_2$ ,  $2_3$  and  $2_4$ , with respect to the translation direction given by  $\vec{T}_2$  for representatives of the sets  $V_2(T_2)$  and  $V_4(T_2)$ .

With

$$\begin{aligned} \vec{2}_1 &= \frac{1}{2}(\tau^2, -1, \tau) & \vec{2}_2 &= \frac{1}{2}(1, -\tau, \tau^2) \\ \vec{2}_3 &= \frac{1}{2}(-1, -\tau, \tau^2) & \vec{2}_4 &= \frac{1}{2}(-\tau^2, -1, \tau) \end{aligned} \quad (35)$$

we obtain the translation lengths  $-\tau'\vec{T}_2$ ,  $\vec{T}_2$  and  $\tau\vec{T}_2$ .

Thus the following admissible translations along a two-fold axis lead to distinct extended symmetry systems:  $T = \tau'^2\vec{T}_2$ ,  $-\tau'\vec{T}_2$ ,  $\vec{T}_2$ ,  $\tau\vec{T}_2$  and  $\tau^2\vec{T}_2$ . Among these,  $-\tau'\vec{T}_2$ ,  $\vec{T}_2$ ,  $\tau\vec{T}_2$  are also special translations.

In summary, the following admissible and special translations correspond to distinct extended symmetry systems for  $(I, v_3)$ :

Direction	admissible	special
$\vec{T}_5 = (1, 0, \tau)$	$-\frac{\tau'}{2}\vec{T}_5, \frac{1}{2}\vec{T}_5, \frac{\tau}{2}\vec{T}_5, \vec{T}_5, \frac{\tau^2}{2}\vec{T}_5$ and $\tau\vec{T}_5$	
$\vec{T}_3 = (0, \tau', \tau)$	$\frac{1}{2}\vec{T}_3, \frac{\tau}{2}\vec{T}_3, \vec{T}_3, \frac{\tau^2}{2}\vec{T}_3$ and $\tau^2\vec{T}_3$	
$\vec{T}_2 = (\tau, 0, 0)$	$\tau'^2\vec{T}_2$ and $\tau^2\vec{T}_2$	$-\tau'\vec{T}_2, \tau\vec{T}_2, \vec{T}_2$

Table 3: *Admissible and special translations corresponding to distinct extensions of the symmetry system  $(I, v_3)$ .*

This concludes our analysis of admissible translations for the symmetry systems  $(I, v_j)$ ,  $j = 1, 2, 3$ , and Tables 1 – 3 provide an exhaustive list of admissible translations corresponding to distinct extensions of these symmetry systems.

We conclude this section with a remark on the relation of these results to previous approaches. In [11] it has been shown that affine extensions of the non-crystallographic Coxeter group  $H_3$ , which contains the icosahedral group  $I$  as a subgroup, can be obtained via an extension of the Cartan matrix that encodes the geometry of the associated root system. Since the root system of  $H_3$  corresponds to vectors pointing to the vertices of an icosidodecahedron, this case is related to our symmetry system  $(I, v_3)$ . The translation obtained in [11] corresponds to the special translations  $T_2$  for this symmetry system. The other admissible and special translations along a two-fold axis obtained here have not been derived previously, but can be obtained in the framework adopted in [11] by relaxing the symmetry condition on the extended Cartan matrix; however, none of the other translations for  $(I, v_3)$ , and none of the results for  $(I, v_1)$  and  $(I, v_2)$  which are associated with start configurations that do not have the properties of a root system, can be obtained with the methodology in that reference.

## 4 Point configurations associated with affine extended symmetry systems

The actions of the monomials of the affine extended symmetry systems  $(I^T, v_j)$ ,  $j = 1, 2, 3$ , on  $v_j$  generate point sets that are invariant under the action of  $I$ . They have the property that every point is symmetry related to every other point in the set, i.e. every point in the set can be mapped on any other via the extended symmetry group. These point sets are hence associated with affine extended symmetry systems in a similar way as the vertex sets of Platonic solids are associated with finite groups in three dimensions: They are generated by the action of the symmetry group on one element of the set. However, while the action of the full (compact) symmetry group is considered in the case of Platonic solids, in the case of a group that consists of a compact part ( $I$  in this case) and a non-compact part (the

translation operator  $T$  in our setting) we allow for the full action of the compact part only. This restriction of the action of the non-compact part (translation operator) is necessary because the compact part corresponds to a non-crystallographic group, and hence without such a restriction an infinite number of distinct points would be obtained that densely fill  $\mathbb{R}^3$ .

In the first subsection, we explain how finite point sets are obtained from the extended symmetry systems by restricting the action of the translation operator. We construct point sets related to extensions of the symmetry systems  $(I, v_j)$ ,  $j = 1, 2, 3$ , explicitly, and determine the cardinalities of these sets. In the second subsection, we discuss which combinations of start configurations are possible from a symmetry point of view, and we enumerate the corresponding combined point sets.

#### 4.1 Point configurations associated with a single start configuration

Every extended symmetry system  $(I^T, v_j)$ ,  $j = 1, 2, 3$ , generates a point set with overall icosahedral symmetry via the action of its monomials on  $v_j$ .

**Definition 4.1** *For an extended symmetry system  $(I^T, v)$  we call the set of monomials containing up to  $s$  copies of  $T$  the  $s$ -order monomial set  $M^s(I, T)$  associated with  $(I^T, v)$ .*

Note that the action of the full extended symmetry group  $I^T$  on  $v$  corresponds to the action of the collection of all monomials on  $v$ , i.e.  $M^s(I, T)v$  for all  $s \in \mathbb{N}$ . For a crystallographic group  $G$   $M^s(G, T)v$  generates a lattice for appropriate  $T$ , whilst for a non-crystallographic group, such as  $I$ , a set dense in  $\mathbb{R}^3$  is obtained. However, for fixed  $s \in \mathbb{N}$ ,  $M^s(I, T)v$  is a finite point set. We demonstrate this for an example in Fig. 19.

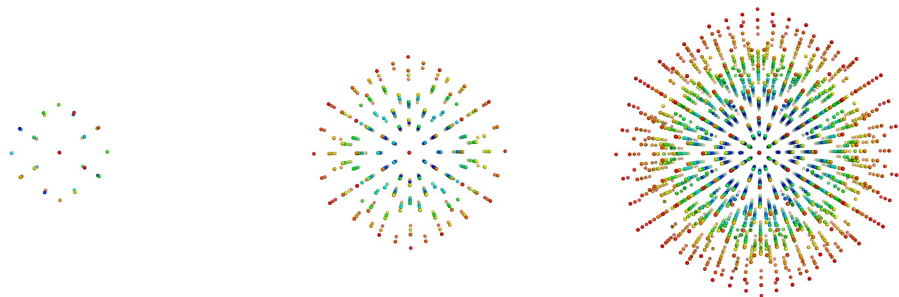


Figure 19: The monomial sets for  $s = 0, 1, 2$  for the extended symmetry system  $(I^T, v_3)$  with  $T = T_2$ .

Since  $M^s(I, T)v$  becomes more dense and spatially extended with increasing  $s$ , only the lowest order monomial sets are relevant for applications describing the symmetries of relatively small objects. This is for example the case for simple viruses, where only a limited number of material boundaries exists. We therefore focus in the remainder of this work on an analysis and classification of the first-order monomial sets of the extended symmetry systems, i.e. on point sets given by  $M^1(I, T)v$ .

We have shown in the previous section that there are in total 41 admissible translations leading to distinct extensions for the symmetry systems  $(I, v_j)$ ,  $j = 1, 2, 3$ . These translations

are distributed (in numbers) among the different start configurations and according to their translation directions as summarised in Table 4.

	5-fold	3-fold	2-fold
icosahedron	3	4	6
dodecahedron	4	3	5
icosidodecahedron	6	5	5

Table 4: *The distribution (in numbers) of admissible and special translations for the three start configurations.*

The first-order monomial sets  $M^1(I, T_i)v_j$ ,  $j = 1, 2, 3$ , corresponding to the translations  $T_i$  in Table 4, can be computed using the information in Tables 1 – 3. To each of the of the 41 extended symmetry systems, i.e. to each of the admissible and special translations in these tables, there corresponds one such set; we display three of them in Fig. 20. These

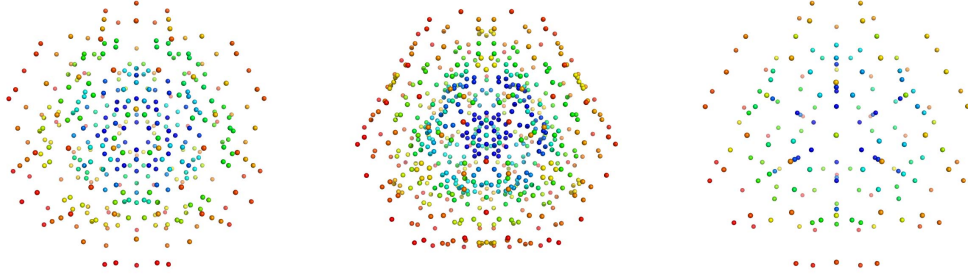


Figure 20: Examples showing three of the 41 configurations in Table 5.

point sets have different cardinalities, i.e. different numbers of distinct elements, and we list the cardinalities of all 41 point sets in Table 5.

## 4.2 Point sets associated with combined start configurations

In the previous section we computed the admissible translations corresponding to the three start configurations, given by the icosahedron, respectively the dodecahedron or the icosidodecahedron. From a group theoretical point of view, it is possible to use combined start configurations provided that all components have the same admissible translation, as stated in the following proposition.

**Proposition 4.2** *Let  $T$  be an admissible translation for the symmetry system  $(G, v)$  and let  $cT$  with  $c \in \mathbb{R}$  be an admissible translation for the symmetry system  $(G, w)$ . Then  $T$  is an admissible translation for the symmetry system  $(G, v + \frac{1}{c}w)$ .*

*Proof:* Let  $cT$  with  $c \in \mathbb{R}$  be an admissible translation for the symmetry system  $(G, w)$ . Then  $T$  is admissible for  $(G, \frac{1}{c}w)$ . Moreover, since both symmetry systems have  $G$  as a symmetry group, the start configurations generated from both  $v$  and  $\frac{1}{c}w$  are invariant under

Icosahedron		Dodecahedron		Icosidodecahedron	
Translation	Cardinality	Translation	Cardinality	Translation	Cardinality
$-\tau'\vec{T}_5$	116	$\tau'^2\vec{T}_5$	200	$-\frac{1}{2}\tau'\vec{T}_5$	290
$\vec{T}_5$	85	$-\tau'\vec{T}_5$	172	$\frac{1}{2}\vec{T}_5$	242
$\tau\vec{T}_5$	116	$\vec{T}_5$	172	$\frac{1}{2}\tau\vec{T}_5$	242
		$\tau\vec{T}_5$	200	$\vec{T}_5$	360
				$\frac{1}{2}\tau^2\vec{T}_5$	290
				$\tau\vec{T}_5$	360
$-\tau'\vec{T}_3$	192	$-\tau'\vec{T}_3$	252	$\frac{1}{2}\vec{T}_3$	362
$\vec{T}_3$	164	$\vec{T}_3$	191	$\frac{1}{2}\tau\vec{T}_3$	374
$\tau\vec{T}_3$	164	$\tau\vec{T}_3$	252	$\vec{T}_3$	600
$\tau^2\vec{T}_3$	192			$\frac{1}{2}\tau^2\vec{T}_3$	362
				$\tau^2\vec{T}_3$	600
$-\tau'\vec{T}_2$	342	$\tau'^2\vec{T}_2$	590	$\tau'^2\vec{T}_2$	710
$2\tau'^2\vec{T}_2$	272	$2\tau'^2\vec{T}_2$	332	$-\tau'\vec{T}_2$	552
$\vec{T}_2$	272	$\vec{T}_2$	590	$\vec{T}_2$	361
$-2\tau'\vec{T}_2$	212	$-2\tau'\vec{T}_2$	344	$\tau\vec{T}_2$	552
$2\vec{T}_2$	212	$2\vec{T}_2$	332	$\tau^2\vec{T}_2$	710
$2\tau\vec{T}_2$	272				

Table 5: *The cardinalities of the sets  $M^1(I, T_m)v_n$  for the 41 extended symmetry systems  $(I^{T^m}, v_n)$  ( $n = 1, 2, 3$ ).*

$G$ , and hence so is also the start configuration generated by their sum, which proves the claim.

From Table 4 we can readily infer the number of possible combined start configurations. There are 342 combinations involving two of the original start configurations; 102 possibilities for admissible translations along 5-fold axes, 85 for admissible translations along 3-fold axes and 155 for admissible translations along 2-fold axes.

## 5 Applications in virology

Since viruses use symmetry for the organisation of their capsids, it is reasonable to explore whether they also use symmetry for the organisation of their full three-dimensional structure from the capsid area down to the innermost density of nucleic acid. Since the extended symmetry systems derived here are the most generic mathematical objects that extend icosahedral symmetry by a non-compact part, one should expect that if viruses use symmetry for their organisation then their structures should be describable in terms of these extended symmetry groups.

In order to determine which of the point sets and hence which of the affine extended symmetry systems provides a blueprint for a given virus, we start by considering the outside of the viral capsid and compare it with the point sets in our classification by considering, in the first instance, only those points with the largest distance from the centre. We will refer

to these points as the *outer layer* of the point set. The following lemma helps to reduce the number of operations that need to be performed.

**Lemma 5.1** *There are in total 26 different outer layers in the 41 point configurations and their combinations.*

*Proof:* For an affine extended symmetry system  $(I^T, v_j)$ ,  $j = 1, 2, 3$ , let  $T_j$  denote a translation along the vector  $v_j$ , i.e.  $T_j(x) := x + v_j$  for  $x \in \mathbb{R}^3$ . The point set associated with the extended symmetry system  $(I^T, v_j)$  contains the set  $M^1(I, T)v_j$ . This set is given by the monomials of the form  $i_1 T i_2$  acting on  $v_j$ , where  $i_k$ ,  $k = 1, 2$ , denote arbitrary elements in  $I$ . However,  $i_1 T i_2 v_j = i_1 T i_2 T_j 0$ , where 0 denotes the origin (centre of the point set), and we can hence express these monomials in terms of the translation operator  $T_j$ . The outer layer of the point set is given by those monomials in which  $i_2$  and  $T_j$  combine to a translation  $\tilde{T}_j$  such that the vectors corresponding to  $T$  and  $\tilde{T}_j$  both point to corners of the fundamental domain of the symmetry group as shown in Fig. 21. This is due to the fact that

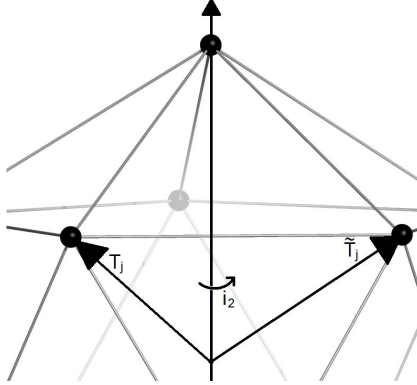


Figure 21: A graphical representation of the locations of  $T$  and  $\tilde{T}_j$  within the fundamental domain of the icosahedral group.

in that constellation these two translations add up to maximal effect. The points forming the outer layer of the point set are hence given by  $i_1 T \tilde{T}_j 0$ . Since translations are commutative, these monomials are the same as  $i_1 \tilde{T}_j T 0$ , and the roles of  $T$  and  $\tilde{T}_j$  can be interchanged. This implies that the outer layer of a point set corresponding to an admissible translation along a  $n$ -fold axis ( $n = 2, 3, 5$ ) and a start configuration with vertices on an  $m$ -fold axes ( $m = 2, 3, 5$ ) of icosahedral symmetry has the same outer layer as a point set corresponding to an admissible translation along the  $m$ -fold axis and a start configuration with vertices on an  $n$ -fold axis of icosahedral symmetry. From Table 4 it can be seen that there are thus 26 different outside layers in the point sets corresponding to the three start configurations.

We next consider the case of combined start configurations, i.e. of extended symmetry systems  $(G^T, v + \frac{1}{c}w)$ , and assume without loss of generality that  $c > 1$ . By definition, the associated point set corresponds to the union of the point sets associated with  $(G^T, v)$  and  $(G^T, \frac{1}{c}w)$ . Since  $c > 1$ , the outer layer of the combined set consists only of points from  $(G^T, v)$ , and we are hence in the scope of the case we already discussed. This completes the proof.

As a consequence of this lemma, we have in a first instance to decide which, if any, of the 26 different configurations describes the outside of the virus we are interested in. Since these 26 configurations are very different, this task can easily be performed and leads to a unique result. For example, for a test virus such as Pariacoto virus, an insect virus with a quasi-equivalent  $T = 3$  structures [17], only 3 of the 41 classified symmetry systems show reasonable matches. These correspond to the red, blue and green vertices in Fig. 22 shown superimposed on the crystal structure of Pariacoto virus which is available as a pdb-file (pdb-ID 1F8V) from the VIPER website [19]. A simple visual comparison shows that whilst the

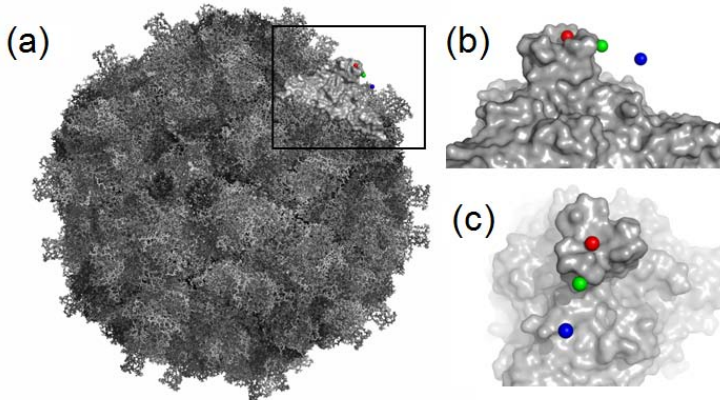


Figure 22: (a) The crystal structure of Pariacoto virus with a trimer highlighted in the upper right-hand corner. (b)&(c) showing close-ups of that trimer, with red points corresponding to the model identified as the outer layer for Pariacoto virus. The green and blue points represent symmetry systems with outer layers closest to the red points; a comparison with the data shows that these are not suitable for the description of Pariacoto virus.

red dots are located on the most radial distant features of the capsid proteins, the green and blue dots do not fit in a meaningful way with the structure. The red dots correspond to the outer layer of points given by the symmetry system  $(I, v_3)$ , with  $v_3$  of length  $\tau$ , extended by the translation  $\frac{\tau'}{2}T_5$ .

In a next step we have to consider all point sets with combined start configurations that have an outer layer of points coinciding with the one we have identified. In the case of Pariacoto virus there are 12 such configurations. We apply the scaling factor associated with the outer layer, i.e. the red points in Fig. 22, to all other symmetry related points in these 12 configurations and compare with the data. For only one of them, corresponding to the symmetry system  $(I, v_3 + \frac{\sqrt{(3)}}{2}v_2)$  extended by the translation  $\frac{\tau'}{2}T_5$ , we find a spread of points that remarkably fits around all molecular boundaries of Pariacoto virus. This implies that this virus has assembled to maximise symmetry in three dimensions, and that icosahedral symmetry occurs on different radial levels orchestrated by this new symmetry principle described here. A more extensive analysis of where these points are situated with respect to the molecular components of this and other viruses will be discussed in [18], where we also show that this approach predicts the organisation of the viral RNA within the bacteriophage MS2 [14, 15, 16, 20]. Remarkably, all viruses we have investigated to date follow the blueprints derived here, implying that it is a previously unrecognised general principle in

virus architecture.

## 6 Discussion

We have classified those extensions of icosahedral symmetry by a translation operator that give rise to lattice-like point sets with geometric properties similar to those of quasi-lattices. From a geometric point of view, such extended groups are associated with nested point sets with icosahedral symmetry at all radial levels in a similar way as the vertex sets of the icosahedron and the dodecahedron are associated with icosahedral symmetry: Both are generated via the action of a symmetry group on one member of the set. These affine extended symmetry systems are hence generic mathematical structures for the description of objects exhibiting icosahedral symmetry at different radial levels, and they predict the spacings of these radial levels as well as their individual organisations. Given the recognised role of icosahedral symmetry in the organisation of viral capsids, it is reasonable to assume that viruses maximise the use of symmetry in their overall organisation. A test on a number of examples, the details of which will be presented elsewhere [18], confirms this conjecture.

The observation that viruses use symmetry for their structural organisation on all radial levels has a plethora of implications. For example, it can be invoked to model the constraints imposed by the co-assembling RNA on the assembly of viral capsids from their protein building blocks. For example, we show in [21] that the constraints implied by the new symmetry principle can be formulated as a Hamiltonian path approach, hence extending earlier work that models the assembly of the viral capsids based on the tiling approach alone [22, 23]. Moreover, the symmetry principle implies geometric constraints on the structural organisation of the capsid proteins.

## Acknowledgements

RT has been supported by an EPSRC Advanced Research Fellowship. TK has been supported by the EPSRC grant GR/T26979/01. We would like to thank Professor Peter Stockley for a careful reading of the manuscript.

## References

- [1] F.H.C. Crick and J.D. Watson, The structure of small viruses *Nature* **177**, 473–475 (1956).
- [2] Caspar, D.L.D & Klug, A. (1962) Physical Principles in the Construction of Regular Viruses. *Cold Spring Harbor Symp. Quant. Biol.* **27**, 1–24.
- [3] Rayment, I., et al. (1982), *Nature* **295**, pp. 110.
- [4] Liddington, R.C. et al. (1991), *Nature* **354**, pp. 278.
- [5] Twarock, R. (2004), A tiling approach to virus capsid assembly explaining a structural puzzle in virology, *J. Theor. Biol.* **226**, pp. 477.

- [6] Twarock, R. (2005) The architecture of viral capsids based on tiling theory, *J. Theor. Medicine* **6**, 87–90.
- [7] Keef, T. & Twarock, R. (2007), Blueprints for viral capsids in the family of Papovaviridae, submitted to *J. Theor. Biol.*
- [8] Senechal, M. (1996) *Quasicrystals and Geometry*, Cam. Univ. Press.
- [9] Shechtman, D., Blech, I., Gratias, D. & Cahn, J.W. (1984) Metallic phase with long-range order and no translational symmetry. *Phys. Rev. Lett.* **53**, 1951–1953.
- [10] R. Twarock (2002) *New group structures for carbon onions and carbon nanotubes via affine extensions of noncrystallographic Coxeter groups*, *Phys. Lett. A* **300** 437–444.
- [11] J. Patera and R. Twarock, *Affine extensions of noncrystallographic Coxeter groups and quasicrystals*, *J. Phys. A* **35** 1551–1574, (2002).
- [12] Janner, A. (2006) Towards a classification of icosahedral viruses in terms of indexed polyhedra, *Acta Crystallographica A* **62**, 319.
- [13] Janner, A. (2006) Crystallographic structural organization of human rhinovirus serotype 16, 14, 3, 2 and 1A, *Acta Crystallographica A* **62**, 270.
- [14] Valegard, K., Liljas, L., Fridborg, K. & Unge, T. (1990) The three-dimensional structure of the bacterial virus MS2, *Nature* **345**, 36.
- [15] Valegard, K., Murray, J.B., Stockley, P.G., Stonehouse, N.J. & Liljas, L., (2002) Crystal structure of a bacteriophage RNA coat protein operator system. *Nature* **371**, 623.
- [16] Golmohammadi, R., Valegard, K., Fridborg, K. & Liljas, L. (1993) The refined structure of bacteriophage MS2 at 2.8 Å resolution. *J. Mol. Biol.* **234**, 620.
- [17] Tang, L., Johnson, K., Ball, L., Lin, T., Yeager, M. & Johnson, J. (2001) *Nature Struct. Biol.* **8**, 77–83.
- [18] Keef, T., Toropova, K., Ranson, N.A., Stockley, P.G., & Twarock, R. (2007) *A new paradigm for symmetry reveals hidden features in the architecture of simple viruses*, in preparation.
- [19] Reddy, V.S., Natarajan, P., Okerberg, B., Li, K., Damodaran, K.V., Morton, R.T., Brooks, C.L. 3rd, Johnson, J.E. (2001) Virus Particle Explorer (VIPER), a website for virus capsid structures and their computational analyses, *J Virol.* **75**, 11943–7.
- [20] Toropova, K., Basnak, G., Twarock, R., Stockley, P.G. & Ranson, N.A. (2007) *The three-dimensional structure of genomic RNA in bacteriophage MS2: Implications for assembly*, to appear in *J. Mol. Biol.*
- [21] Grayson, N., Keef, T., Severini, S. and Twarock, R. (2007) *Assembly pathways for bacteriophage MS2 based on a Hamilton path approach*, in preparation
- [22] Keef, T., Taormina, A. and Twarock, R. (2005) *Assembly Models for Papovaviridae based on Tiling Theory*, *Phys. Biol.* **2**, 175–188.

- [23] Keef, T., Micheletti, C. and Twarock, R. (2006) *Master equation approach to the assembly of viral capsids*, *J. Theor. Biol.* **242**, 713-21.
- [24] Bamford, DM, Burnett, RM & Stuart, DI (2002) *Evolution of Viral Structure Theor. Pop. Biol.* **61**, 461; Bamford, D.H., Grimes, J.M. & Stuart D.I (2005) *What does structure tell us about virus evolution?* *Curr. Opin. Struct. Biol.* **15**, 655.